Supplemental Material

Supplemental Information for: Randomized trial of calcipotriol combined with 5-fluorouracil for skin cancer precursor immunotherapy.

Supplemental Methods

Animal Studies

For skin cancer studies, 4-6 week-old mice were treated with a standard skin chemical carcinogenesis protocol (1). The back skin of the animals was shaved and treated with a single dose of 50 μg DMBA (carcinogen) followed by a twice-weekly application of 6 μg TPA (promoting agent) for 15 weeks. Mice were monitored for 10-15 weeks following the last TPA treatment. Time to tumor onset, tumor count and animal weight were documented and photographs taken. In the first set of experiments, age- and gender-matched wild-type (Wt) and TSLPR^{-/-} mice on the C57BL/6 background (a gift from Warren Leonard, NIH, Bethesda, MD) were treated with calcipotriol (80 nmol in 200 μl EtOH; Sigma) or carrier only (EtOH) on back skin three times a week during the DMBA-TPA treatment period. In a transient TSLP induction experiment, age- and gender-matched Wt mice on the FVB background were treated with calcipotriol (80 nmol in 20 μl EtOH) or EtOH alone applied to the ears once a day for three consecutive days at the first sign of skin tumor development in response to DMBA-TPA treatment. In experiments using a cream/ointment carrier, age- and gender-matched Wt animals on the FVB background were treated with combinations of 0.005% calcipotriol ointment (Taro Pharmaceuticals, Ossining, NY) plus 5% 5-FU cream (Taro Pharmaceuticals), Vaseline (petroleum jelly; Fougera) plus 5% 5-FU cream, 0.005% calcipotriol ointment plus moisturizing cream (Curel, Cincinnati, OH), or Vaseline plus moisturizing cream at 1:1 weight ratio once a day for two consecutive days during the early stages of skin tumor development in DMBA-TPA treated mice. Serum TSLP concentrations were measured in blood obtained 24 hours after the final treatment in the calcipotriol/EtOH, treatment group, using a mouse TSLP ELISA kit (BioLegend, San Diego, CA). We used log-rank test for time to tumor onset and two-tailed unpaired Student's t test for other measurements as the tests of significance between the study groups.

Tissue Studies

To determine the induction of TSLP by calcipotriol and investigate other cellular and molecular changes upon calcipotriol plus 5-FU versus Vaseline plus 5-FU treatment, we obtained optional 4 mm punch biopsies of the normal skin and actinic keratosis before and after treatment. Hematoxylin and Eosin (H&E)-stained skin biopsy specimens were scored in a blinded manner by dermatopathology experts according to the Banff 2007 working classification (2). Established criteria were used for grading the degree of skin inflammation and the involvement of epidermis and adnexal structures. In addition, the immune infiltrate in the skin after treatment

was characterized using immunohistochemical staining (For antibodies, see Supplemental Table 6A). Briefly, formalin-fixed paraffin-embedded 5µm tissue sections were stained using the Ventana/Roche Discovery Ultra staining platform (Tucson, AZ). Tissue sections were deparaffinized and antigen retrieval performed when needed. Sections were incubated with primary antibodies for 16 minutes, followed by horseradish peroxidase (HRP) conjugated secondary antibodies. Sections were then stained either with Ventana's Discovery ChromoMap DAB or Discovery Purple staining kits. Sections were counterstained with hematoxylin. Protein and gene expression were measured using tissue immunofluorescence and qRT-PCR assays on RNA from the biopsied samples, respectively (For primers, see Supplemental Table 6B).

Quantitative RT-PCR

Total RNA from participants' actinic keratosis biopsies was isolated using an AllPrep DNA/RNA Micro Kit (Qiagen, Venlo, Netherlands) and its quantity was determined using a NanoDrop ND-1000 (Nanodrop Technologies, Wilmington, DE). cDNA was synthesized using 100ng of total RNA with Invitrogen SuperScript III Reverse Transcriptase (Life Technologies, Carlsbad, CA) and amplified with iTaq™ Universal SYBR® Green Supermix (Bio-Rad Laboratories, Hercules, CA) using a LightCycler® 480 System (Roche, Basel, Switzerland). All transcript levels were normalized to *gapdh*.

Immunofluorescent and Special Stains

For immunofluorescent staining, the participants' biopsy samples were embedded directly in OCT Freezing Medium (Sakura Finetek, Torrance, CA) and frozen. Sections were cut at 7µm and incubated with primary followed by secondary antibodies (for the list of antibodies, see Supplemental Table 6A). All slides were counterstained with DAPI nuclear stain (Thermo Fisher Scientific). Eosinophils were selectively stained with Carbol Chromotrope (3) and mast cells stained with toluidine blue (4). For eosinophil staining, formalin-fixed paraffin-embedded 5µm tissue sections were mounted on glass slides and deparaffinized followed by hematoxylin staining for 5 minutes and bluing. Sections were then placed in Carbol Chromotrope staining solution for 30 minutes followed by rinsing in water. Sections were dehydrated, cleared, and mounted.

Image Alignment and Color Normalization

Given the number of input images, we set one of them as our reference image (i.e., fixed image) and the rest as target images (i.e., moving images). In order to have a fair comparison among

images, we first aligned the images spatially. To accomplish this, as the first step in our pipeline, we applied geometric transformations to the moving image so that all the images were aligned to the reference image. This task in computer vision is called image registration; image registration is the process of transforming different sets of data into one coordinate system. Registration is necessary in order to compare or integrate the data obtained from different measurements. We applied Advanced Normalization Tools (ANTs) algorithm to perform our image registration (5). Supplemental Figure 8A shows a general optimization approach in ANTs algorithm. In simple language, the first term (transformation model) is to encourage the objective function for regularization and the second term is to encourage the alignment of the points with similar features. Examples of the registered images are shown in Supplemental Figure 8B. As seen in this figure, there are meaningful differences between the colors of the images, which can occur due to the different sources (e.g., light source). To address this issue and perform color normalization among the images, we selected a number of patches on the reference image and applied a simplified version of the harmonization technique (6, 7); applying this method, to each image, for each of the patches, we computed expected values of the RGB channels as the sample mean of the voxels within each patch. We computed means of the images/patches by the variables as shown in the following tables:

	Red	Green	Blue
Patch#1	R11	G11	B11
Patch#2	R21	G21	B21
Patch#3	R31	G31	B31

(e.g. R1=mean(R11,R21,R31))

Reference image

|	Red	Green	Blue
Patch#1	R12	G12	B12
Patch#2	R22	G22	B22
Patch#3	R32	G32	B32
Mean	R2	G2	B2

Moving image

To perform color normalization on the moving image, we computed proper coefficients for each of the color channels as:

	Red	Green	Blue
Mean	R2/R1	G2/G1	B2/B1

Which were used to rescale the RGB information of the pixels in the moving image. Example of the color-normalized image is shown in Supplemental Figure 8B.
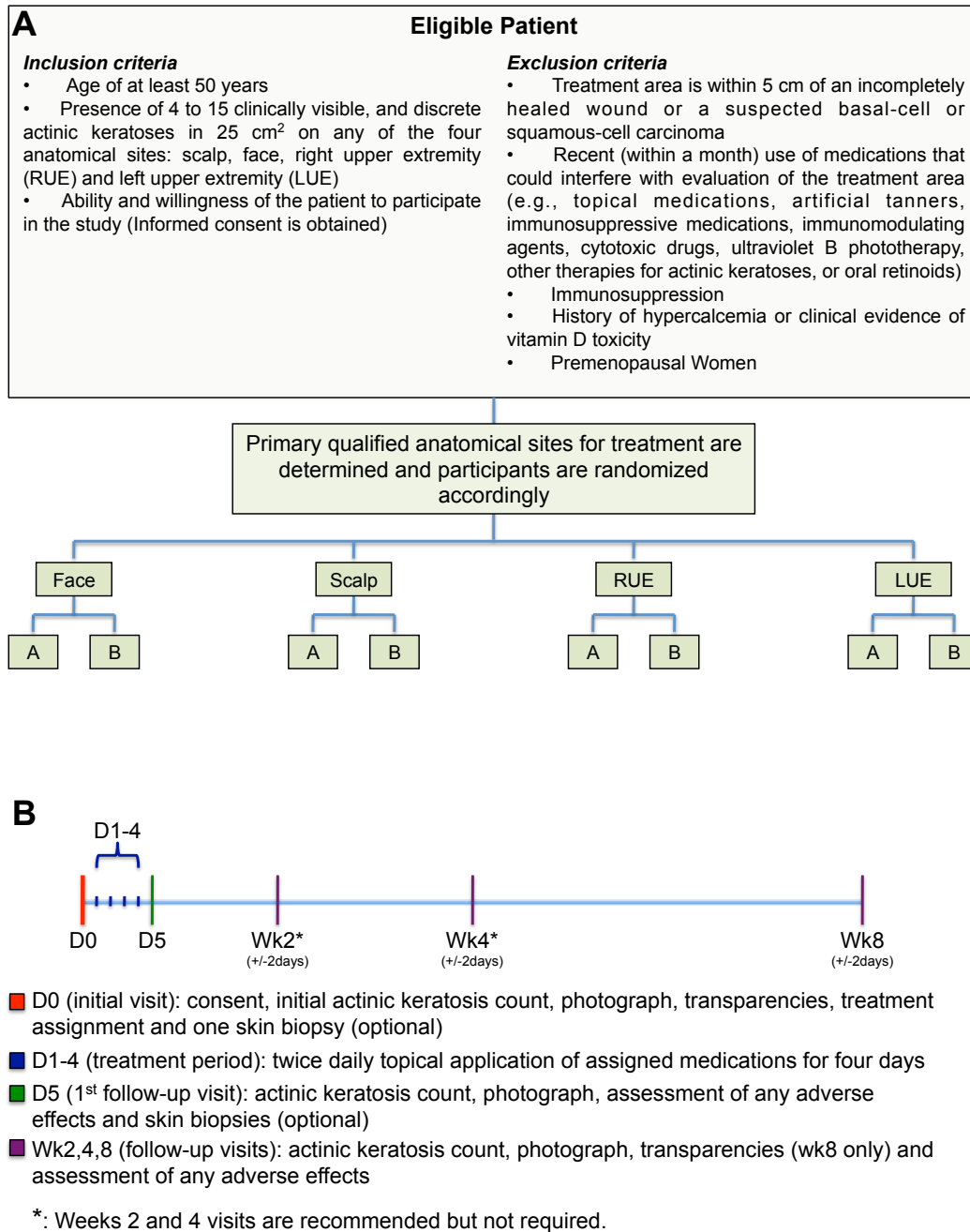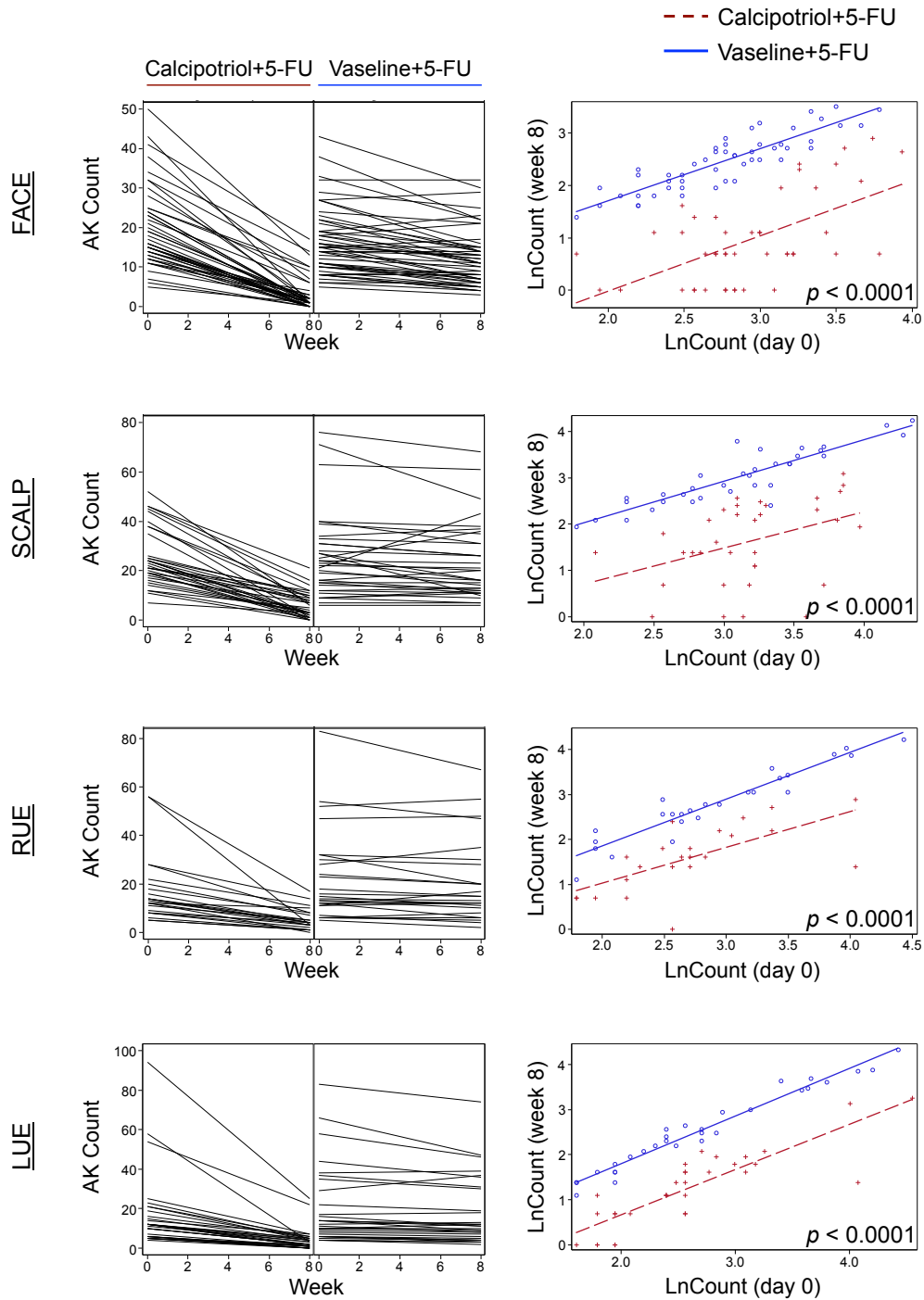
Supplemental Figures
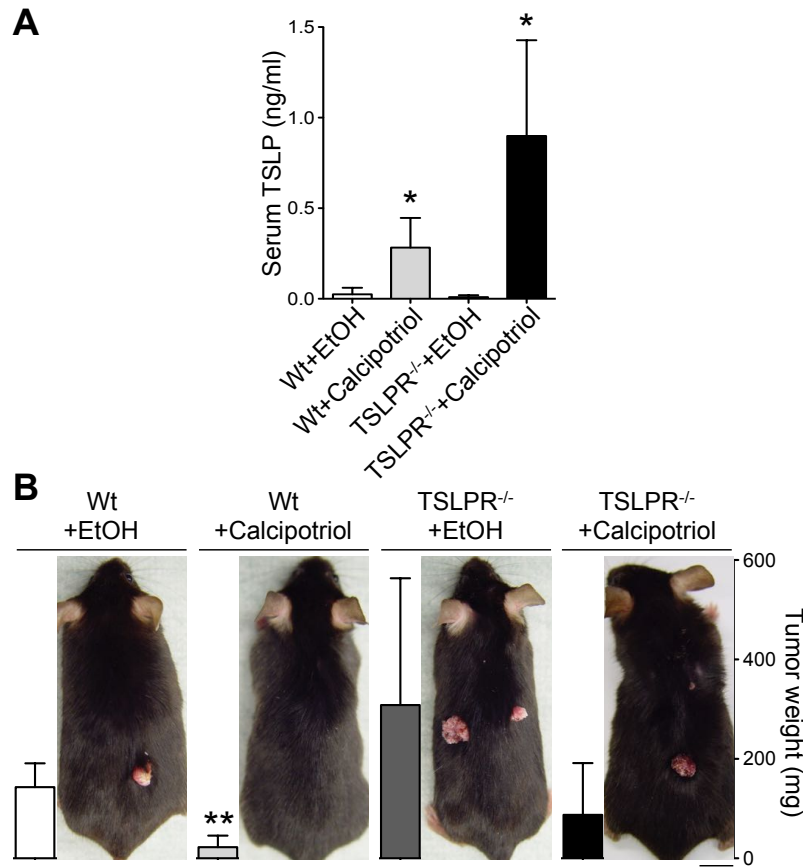
Supplemental Figure 1. TSLP-dependent impact of calcipotriol on skin cancer suppression. (**A**) Wt and TSLPR^{-/-} mice receiving calcipotriol (80 nmol) on their back skin three times a week during DMBA-TPA treatment show elevated serum TSLP levels compared to EtOH-treated groups (*: $p < 0.05$ compared to Wt+EtOH group, Student's *t test*). (**B**) Representative images of the tumor-bearing mice and average weight of the seven largest tumors in each group are shown (**: $p < 0.01$ compared to Wt+EtOH group, Student's *t test*; scale bar = 1 cm).
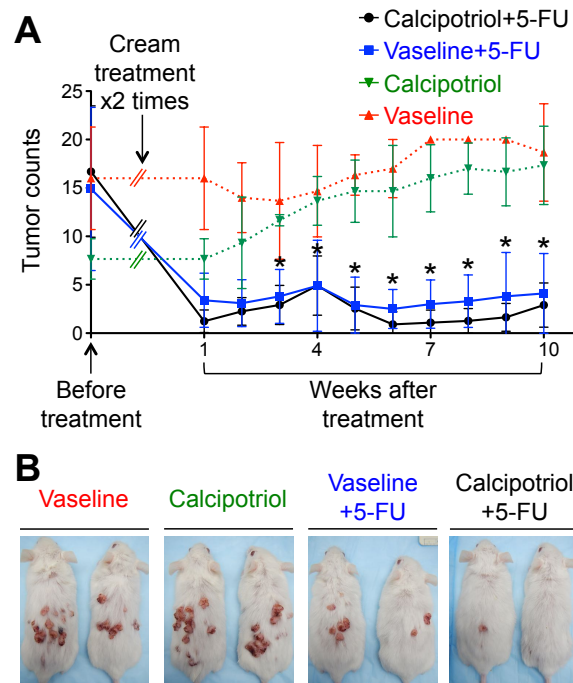
Supplemental Figure 2. Efficacy of calcipotriol ointment as a monotherapy for skin cancer. (**A**) Age- and gender-matched Wt mice were treated with standard DMBA-TPA protocol on their back skin. During the early stages of the skin tumor development, animals were randomized into four groups and treated on the back skin with 0.005% calcipotriol ointment plus 5% 5-FU cream, Vaseline plus 5-FU, calcipotriol plus moisturizing cream (calcipotriol) or Vaseline plus moisturizing cream (Vaseline) once daily for 2 consecutive days. Following this topical treatment, the animals continued to receive TPA biweekly and the tumor counts were monitored (n $\geq$ 5 for each group). Graph shows the number of tumors per mouse over time (*: *p* <0.05 for both calcipotriol plus 5-FU and Vaseline plus 5-FU groups compared to Vaseline group, Student's *t test*). (**B**) Representative pictures of the tumor-bearing mice 10 weeks after the topical treatment are shown (scale bar = 1 cm).

A   **Eligible Patient**

Inclusion criteria
• Age of at least 50 years
• Presence of 4 to 15 clinically visible, and discrete actinic keratoses in 25 cm^2 on any of the four anatomical sites: scalp, face, right upper extremity (RUE) and left upper extremity (LUE)
• Ability and willingness of the patient to participate in the study (Informed consent is obtained)

Exclusion criteria
• Treatment area is within 5 cm of an incompletely healed wound or a suspected basal-cell or squamous-cell carcinoma
• Recent (within a month) use of medications that could interfere with evaluation of the treatment area (e.g., topical medications, artificial tanners, immunosuppressive medications, immunomodulating agents, cytotoxic drugs, ultraviolet B phototherapy, other therapies for actinic keratoses, or oral retinoids)
• Immunosuppression
• History of hypercalcemia or clinical evidence of vitamin D toxicity
• Premenopausal Women

Primary qualified anatomical sites for treatment are determined and participants are randomized accordingly

Face	Scalp	RUE	LUE
A B	A B	A B	A B

B

D1-4

D0   D5   Wk2*   Wk4*   Wk8
            (+/-2days)   (+/-2days)   (+/-2days)

■ D0 (initial visit): consent, initial actinic keratosis count, photograph, transparencies, treatment assignment and one skin biopsy (optional)
■ D1-4 (treatment period): twice daily topical application of assigned medications for four days
■ D5 (1st follow-up visit): actinic keratosis count, photograph, assessment of any adverse effects and skin biopsies (optional)
■ Wk2,4,8 (follow-up visits): actinic keratosis count, photograph, transparencies (wk8 only) and assessment of any adverse effects

*: Weeks 2 and 4 visits are recommended but not required.

Supplemental Figure 3. Clinical study design. (**A**) A set of inclusion and exclusion criteria was applied to screen patients with actinic keratoses for this study. The enrolled participants were examined on day 0 to determine their qualified anatomical sites (face, scalp, right upper extremity (RUE) and/or left upper extremity (LUE)). For participants with more than one qualified anatomical sites, one was selected as the primary site, which was solely used for the randomization purpose. (**B**) The timeline of the clinical visits and treatment regimen are shown.

7

Supplemental Figure 4. Analysis of the primary endpoint while taking into account the baseline number of actinic keratoses. Changes in the number of actinic keratoses on the face, scalp, RUE and LUE from before treatment (day 0) to after treatment (week 8) are plotted. Statistical analysis is performed to determine the significance of treatment effect on natural log

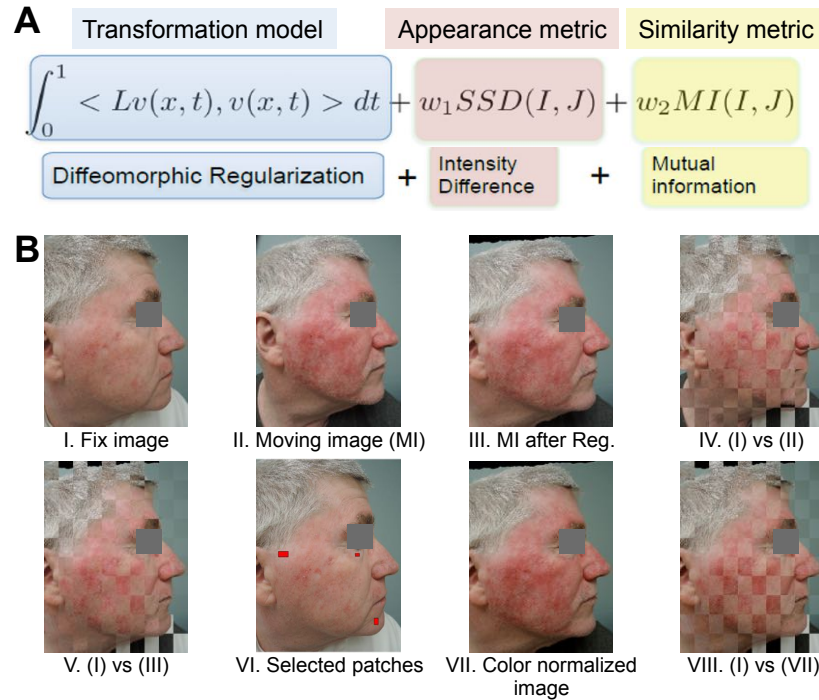transformed actinic keratosis counts after controlling for baseline count, age, and gender of the participants using a mixed random effects model.
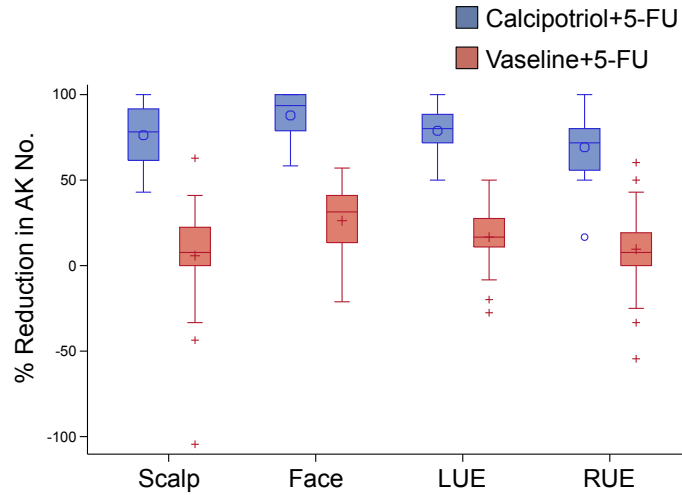
Supplemental Figure 5. Anatomical site differences in response to therapy. The Location*Drug test for fixed effects indicates that the drug effect is consistent among all four anatomical sites (p = 0.3662). The box-and-whisker plots show a similar pattern of efficacy across the anatomical sites.
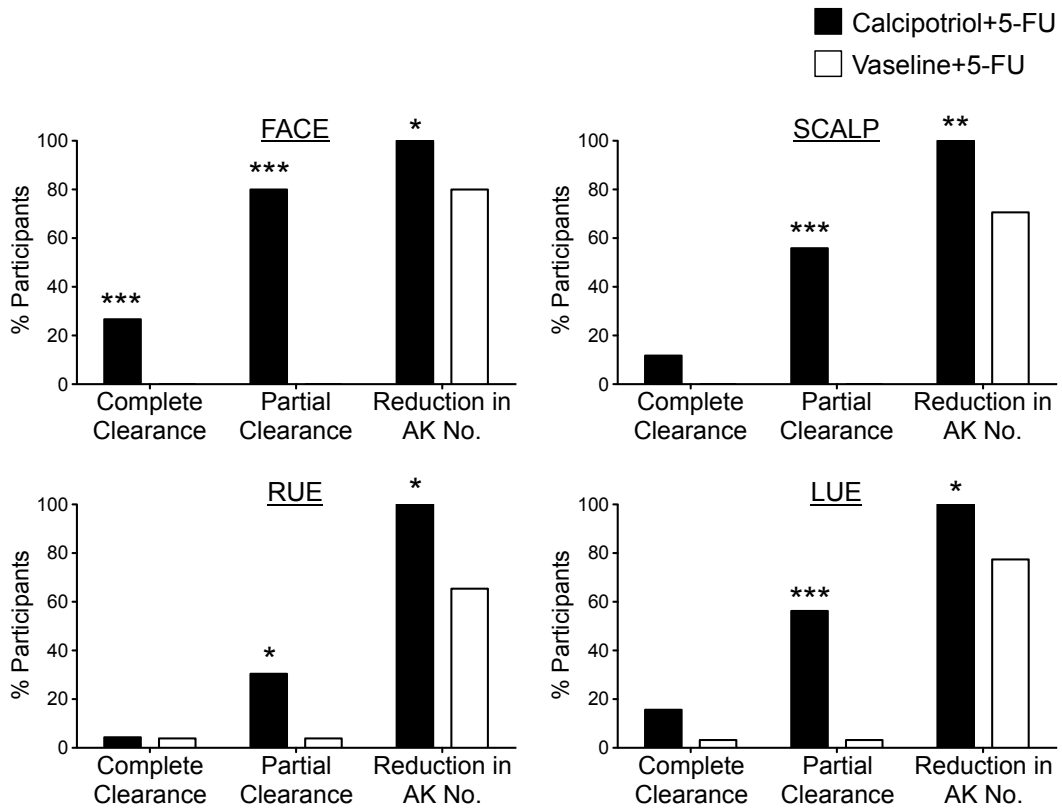
Supplemental Figure 6. Complete and partial clearance and percent reduction rate of actinic keratoses at week 8. Bar graphs show the efficacy outcomes (*secondary endpoints*) for the four anatomical sites treated with calcipotriol plus 5-FU or Vaseline plus 5-FU at week 8 (*: *p* <0.01, **: *p* <0.001, ***: *p* <0.0001; Fisher's exact test).

Calcipotriol+5-FU

	Day 0	Day 5	Week 8
FACE			
SCALP			
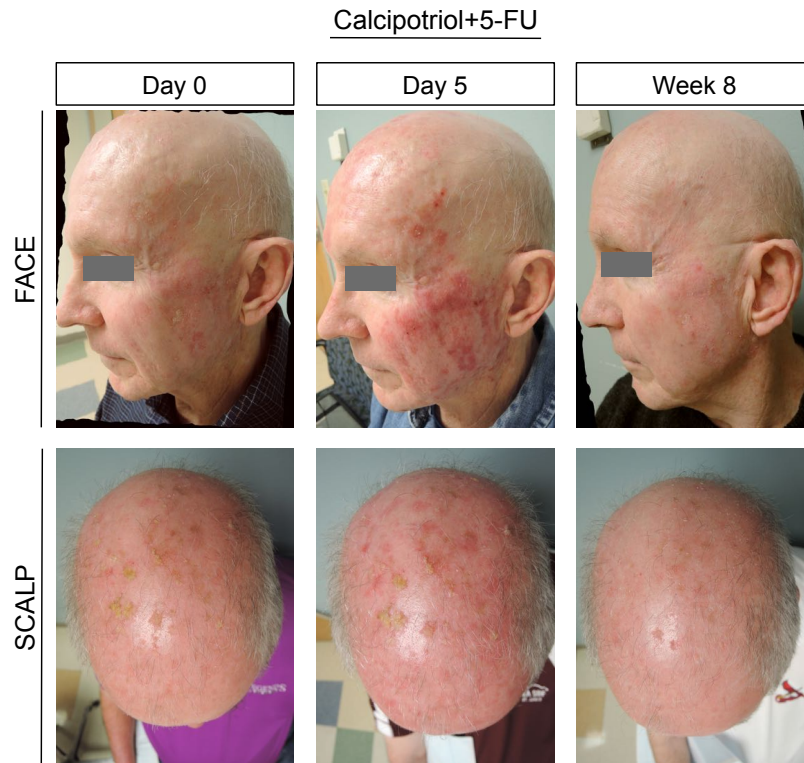
Supplemental Figure 7. Calcipotriol plus 5-FU treatment impact on hypertrophic actinic keratoses. Representative photographs of participants with multiple hypertrophic actinic keratoses on face and scalp who were treated with calcipotriol plus 5-FU combination are shown. Note the intense erythema centered on the lesions at day 5 and a visible improvement in the lesions at week 8. Face photographs are aligned and color normalized.

A

| Transformation model | Appearance metric | Similarity metric |

$$\int_0^1 < Lv(x,t), v(x,t) > dt + w_1 SSD(I,J) + w_2 MI(I,J)$$

Diffeomorphic Regularization + Intensity Difference + Mutual information

B

I. Fix image   II. Moving image (MI)   III. MI after Reg.   IV. (I) vs (II)

V. (I) vs (III)   VI. Selected patches   VII. Color normalized image   VIII. (I) vs (VII)

Supplemental Figure 8. Image registration and color normalization method. (**A**) Advanced Normalization Tools (ANTs) algorithm used to perform image registration (5, 6). In simple language, the first term (transformation model) is to encourage the objective function for regularization and the second term is to encourage alignment of the points with similar features. (**B**) Example reference (B.I) and moving (B.II) images are shown. The registered image of (B.II) is shown in (B.III). The checkerboard visualization of (B.I) and (B.II) images are shown in (B.IV). The checkerboard visualization of (B.I) and (B.III) is shown in (B.V). The selected patches of the reference image used to perform color normalization are shown in (B.VI). The final image, after performing color normalization is shown in (B.VII). Checkerboard representation of (B.I) and (B.VII) is shown in (B.VIII).
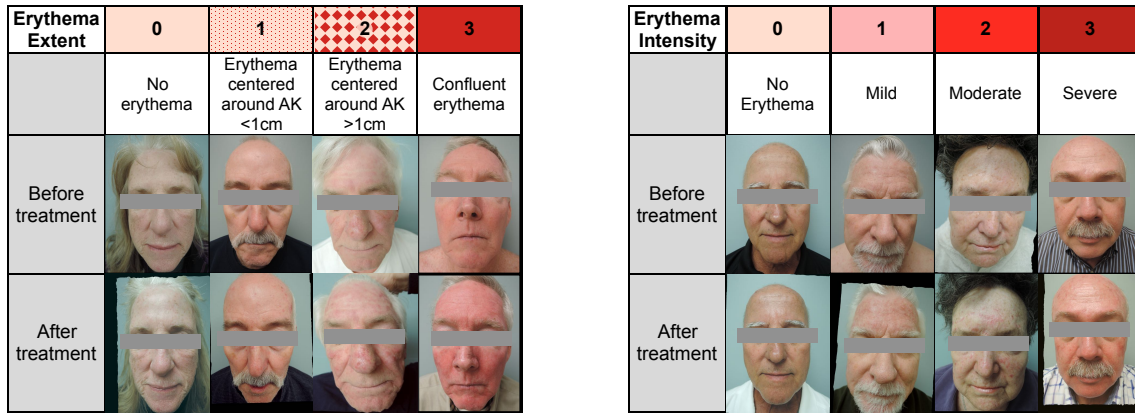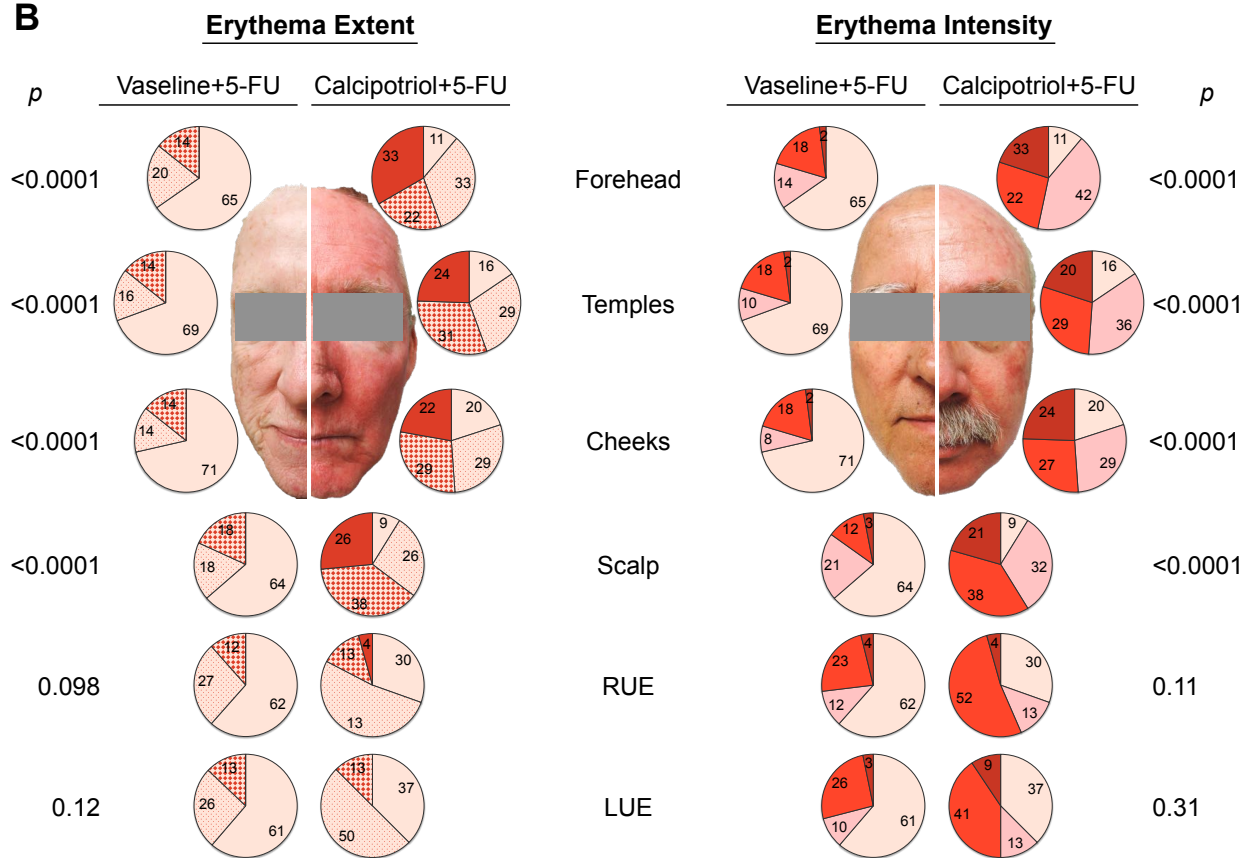
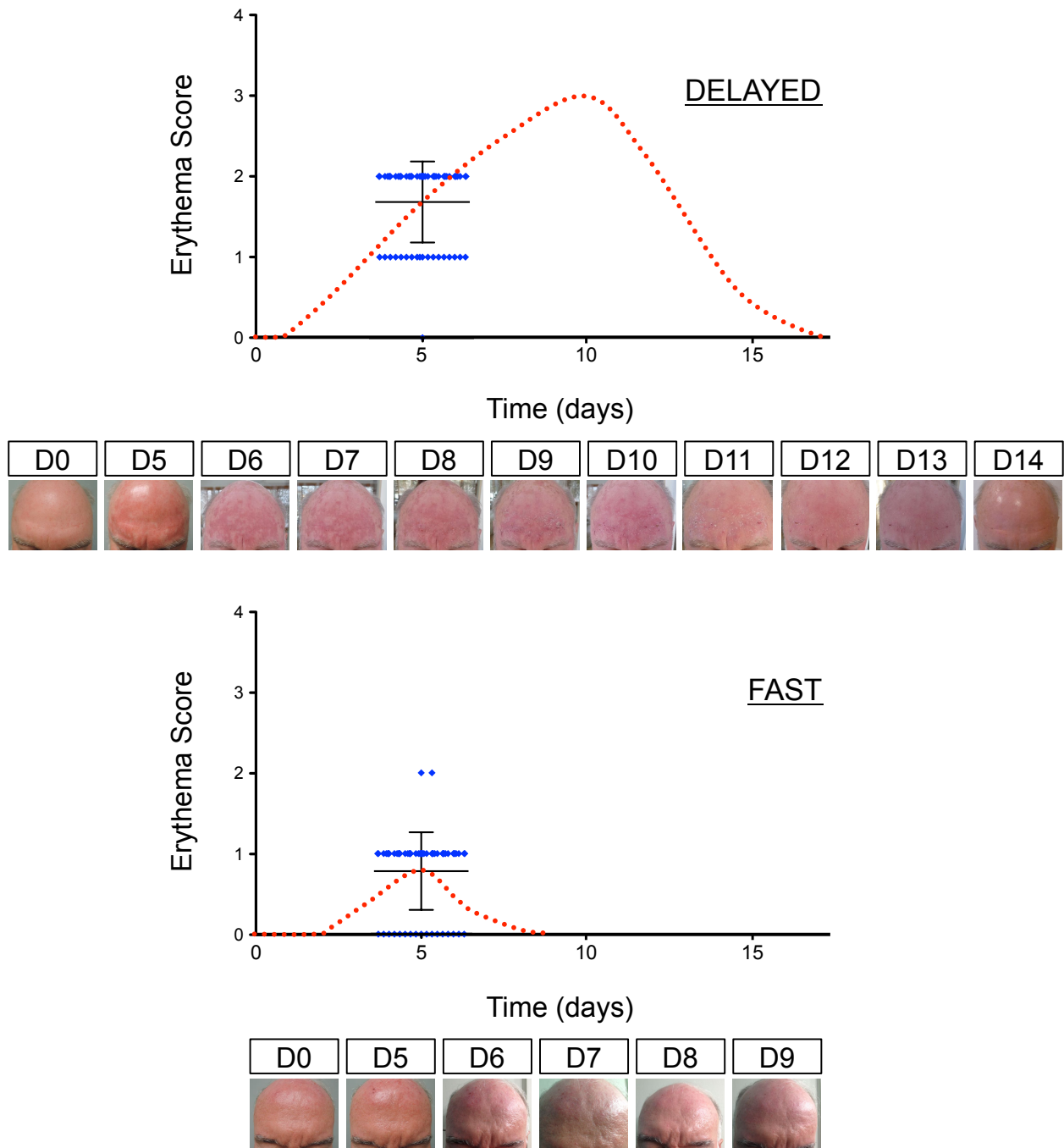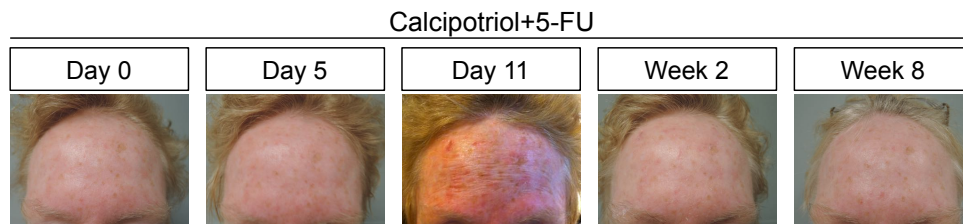**Supplemental Figure 9. Treatment-induced erythema extent and intensity at day 5.** (**A**) Tables show the erythema extent and intensity scales used to score participants' treatment-induced erythema by a trained physician after image alignment and color normalization (Supplemental Figure 8) were performed between day 0 to day 5 photographs. Representative aligned and color normalized before and after photographs for each score are shown. (**B**) Pie charts show the extent and intensity of erythema induced by the treatment on face, scalp, RUE and LUE. For this analysis, face is divided to forehead, temples and cheeks. Note the high

extent and intensity of erythema induced by calcipotriol plus 5-FU at day 5, particularly on the forehead and temples (Fisher's exact test).

Supplemental Figure 10. Erythema resolution patterns. Based on participants' reporting of their skin erythema resolution after treatment, two distinct patterned emerged: (1) Delayed resolution pattern, which implies worsening of the skin redness after treatment with the worst redness and pealing appearing at day 10-11 after treatment, and (2) fast resolution pattern, which denotes a gradual reduction in skin redness right after the treatment was completed (day

5) with no peeling. Erythema scale (Supplemental Table 2) is used to depict the graphical representation of the two patterns. Note that clinical erythema scores at day 5 are shown for participants with delayed versus fast erythema resolution patterns on their respective graphs. Representative photographs of skin erythema resolution on forehead for the delayed and fast groups are shown.

Calcipotriol+5-FU

Day 0	Day 5	Day 11	Week 2	Week 8

Supplemental Figure 11. Delayed immune activation in response to calcipotriol plus 5-FU treatment. Photographs demonstrate the delayed development of erythema (day 11) at the sites of actinic keratoses on the forehead of a participant in calcipotriol plus 5-FU group whose clinical erythema score at day 5 was zero.

Supplemental Figure 12. Resolution of skin reactions by week 2. Representative photographs show the clearance of erythema in calcipotriol plus 5-FU group around the week 2 after treatment (day 0, 5 and week 8 photographs appear in Figure 4A). Note the residual exfoliation present on the skin of the participant in calcipotriol plus 5-FU group at week 2.

Time from the end of treatment
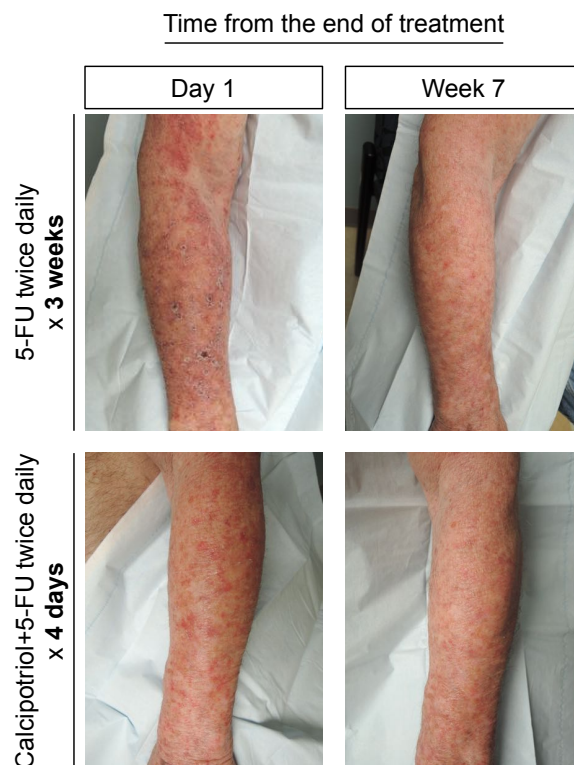
Supplemental Figure 13. Differential skin reactions in response to 4-day calcipotriol plus 5-FU versus 3-week 5-FU treatment. Clinical Photographs show the treated arms of a participant in calcipotriol plus 5-FU group, who had previously experienced a 3-week twice-daily treatment with 5-FU. 5-FU treatment on the RUE was done prior to patient's enrollment into the study for the treatment of actinic keratoses on his LUE. Photographs are taken the day after each treatment is completed (day 1, corresponding to day 5 for the study arm) and 7 weeks later (corresponding to week 8 for the study arm).
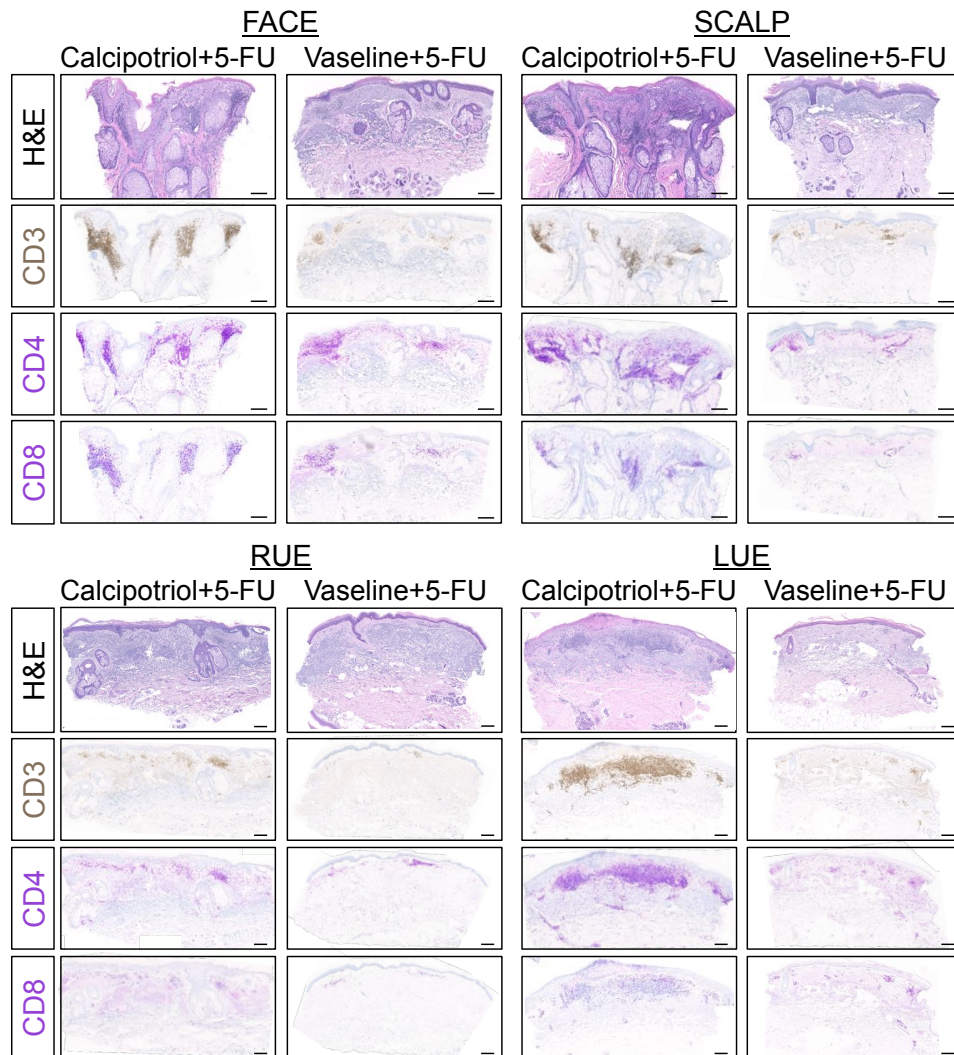
Supplemental Figure 14. T cell mediated immune response to actinic keratoses at day 5. Low magnification images of the H&E, CD3, CD4 and CD8 stained actinic keratosis biopsies at day 5 (shown in Figure 5A) demonstrate the localization, density and extent of T cell infiltrate in the lesions on the four treated anatomical sites in calcipotriol plus 5-FU and Vaseline plus 5-FU groups (scale bars = 200 µm).
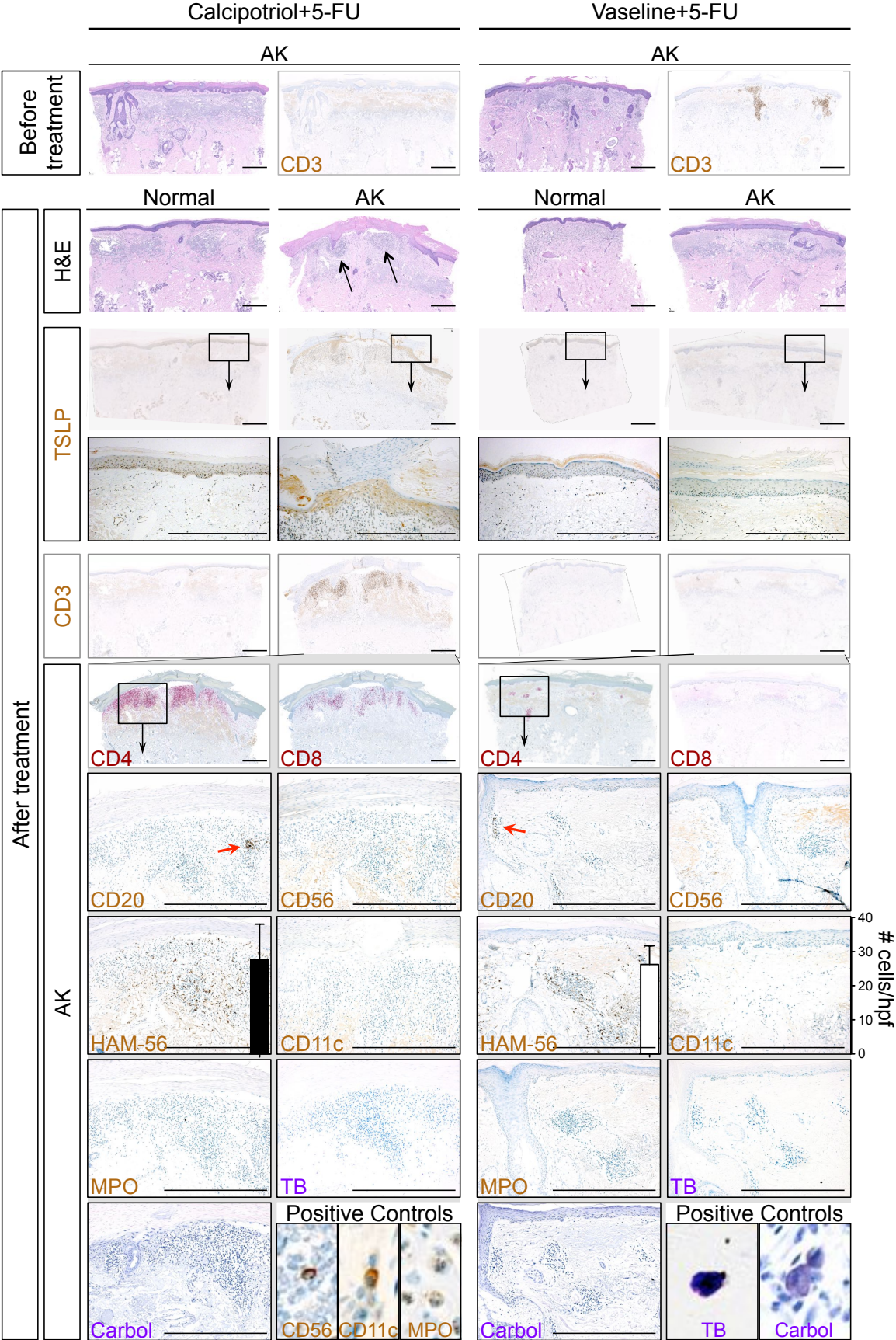
Supplemental Figure 15. Characterization of the immune response to calcipotriol plus 5-FU treatment. Representative images of normal skin and actinic keratoses before and after treatment with calcipotriol plus 5-FU and Vaseline plus 5-FU are shown. Black arrows in H&E-stained tissue section point to the areas of lymphoid aggregate in the calcipotriol plus 5-FU treated actinic keratosis. Immunohistochemical staining for CD3 (before and after treatment), TSLP, CD4 (insets are shown in high-power immunostained images), CD8, CD20 (B cells), CD56 (natural killer cells), HAM-56 (macrophages), CD11c (dermal dendritic cells), Neutrophil myeloperoxidase (MPO), toluidine blue (TB; mast cells) and carbol chromotrope stain (eosinophils) are shown. Red arrows point to the rare cluster of B cells in the treated actinic keratoses. Bar graphs next to images show the average number of HAM-56^{+} dermal macrophages in 10 random high power fields (hpf; $p = 0.7$, Student's *t test*). For cell types not found in the actinic keratoses, positive controls for staining are shown (scale bars = 500 μm).
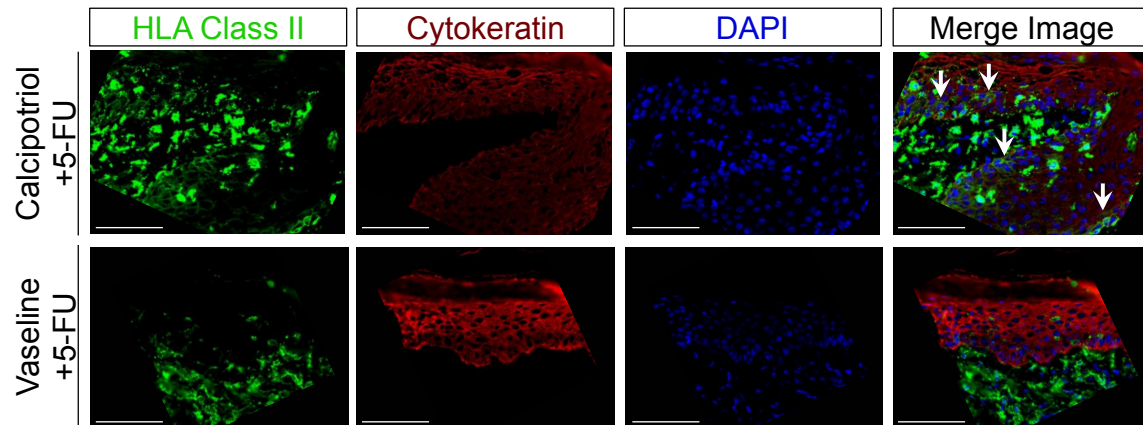
Supplemental Figure 16. HLA class II expression in actinic keratosis at day 5. HLA DP/DQ/DR and cytokeratin stained actinic keratosis biopsies at day 5 are shown. White arrows point to the keratinocytes expressing HLA class II in calcipotriol plus 5-FU treated actinic keratosis (scale bars = 100 μm).
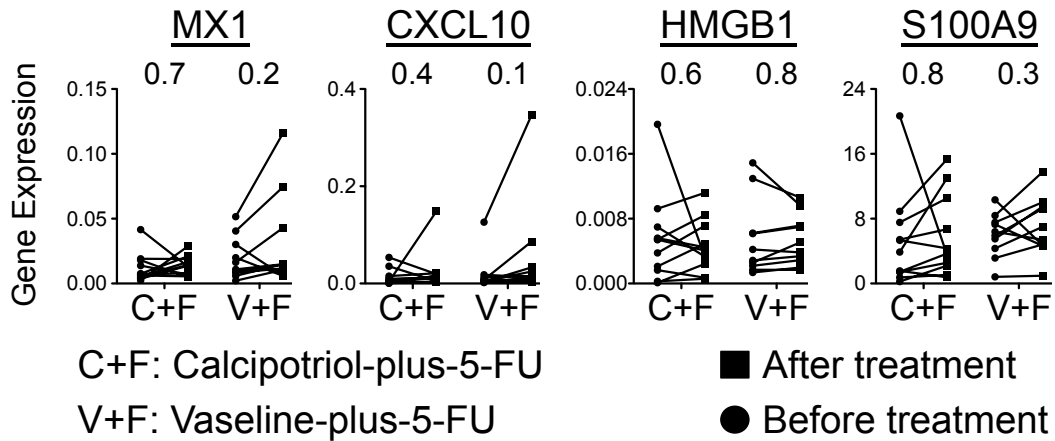
Supplemental Figure 17. Stress signals expression in response to therapy. Graphs demonstrate the relative expression of the immunostimulating genes compared to GAPDH in actinic keratoses before and after treatment with calcipotriol plus 5-FU (n = 11) or Vaseline plus 5-FU (n = 10; paired Student's *t test*).

Supplemental Tables

Supplemental Table 1. Effectiveness of the study treatment compared to participants' previous experience with field treatment for actinic keratosis (AK).

	Calcipotriol+5-FU (n = 64)	Vaseline+5-FU (n = 67)	*p value*
History of AK field treatment, no. (%)	33 (52)	28 (42)	0.26
Current treatment was more effective than previous field treatment(s), no. (%)			
Yes	27 (82)	3 (11)	<0.0001
No/not sure	6 (18)	25 (89)	

Supplemental Table 2. Erythema scale.

Erythema Scale	
0	No erythema
1	Mild erythema
2	Severe erythema with minimal scaling
3	Severe erythema with significant scaling
4	Severe erythema with scaling, crusting, itching and burning

Supplemental Table 3. Clinical erythema scores.

		Calcipotriol+5-FU (n = 64)	Vaseline+5-FU (n = 67)	*p value*
Clinical Assessment on Day 5				
Erythema score per anatomical site, no. (%)				
Face	**0**	1 (2)	13 (26)	<0.0001
	1	8 (18)	35 (70)	
	2	36 (80)	2 (4)	
Scalp	**0**	0 (0)	9 (26)	<0.0001
	1	11 (32)	24 (71)	
	2	23 (68)	1 (3)	
RUE	**0**	1 (4)	9 (35)	<0.01
	1	13 (57)	15 (58)	
	2	9 (39)	2 (8)	
LUE	**0**	2 (6)	10 (32)	<0.01
	1	20 (63)	19 (61)	
	2	10 (31)	2 (6)	

*This table corresponds to Figure 4B.

Supplemental Table 4. Histological grading of immune activation against actinic keratoses after treatment.

(**A**) Criteria used for grading the treated actinic keratosis (AK) biopsies at day 5(2, 8). (**B**) Histological images that are representative of each grade are shown. (**C**) Grades assigned to actinic keratoses in calcipotriol plus 5-FU and Vaseline plus 5-FU groups by dermatopathologist blindly are shown (corresponding to Figure 5B). (**D**) Pie charts compare the pathological grades of the treated actinic keratoses in each treatment group to untreated actinic keratoses (pie charts of the treated groups appear in Figure 5B). Note that pre-treatment samples are independent of post-treatment samples. *P* value was determined by type III test of means in a mixed random effects ANOVA.

A

**Pathological Grades for Immune-Mediated Cutaneous Rejection**

Grade 0: No or rare inflammatory infiltrates.

Grade I: Mild perivascular infiltration. No involvement of the overlying epidermis.

Grade II: Moderate-to-severe perivascular inflammation with or without mild epidermal and/or adnexal involvement (limited to spongiosis and exocytosis). No epidermal dyskeratosis or apoptosis.

Grade III: Dense inflammation and epidermal involvement (significant spongiosis and exocytosis) with epithelial apoptosis, dyskeratosis and/or keratinolysis.
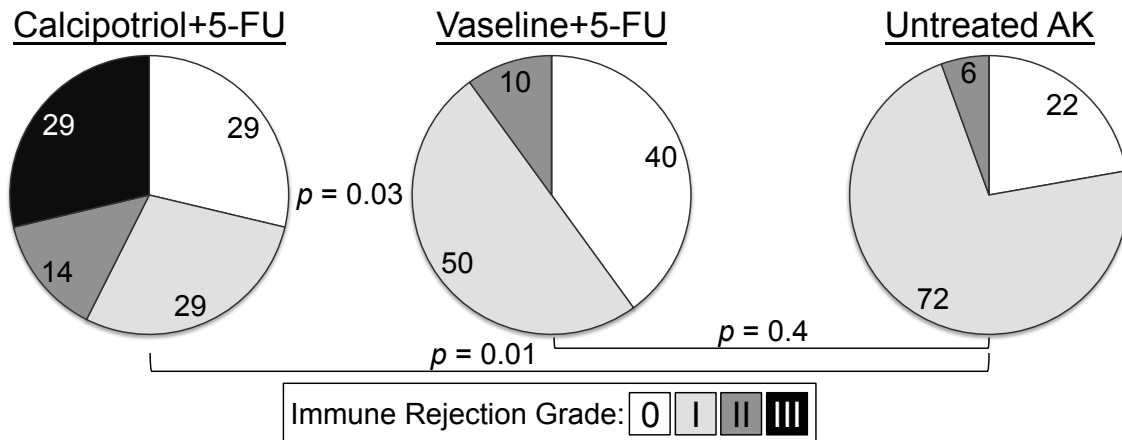
B
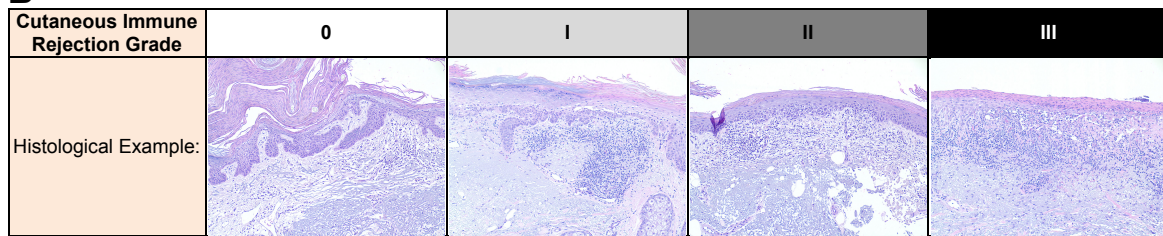
C

	Calcipotriol+5-FU (n = 21)	Vaseline+5-FU (n = 20)	*p value*
Cutaneous Immune Rejection Grade, no. (%)			
0	6 (29)	8 (40)	0.0339
I	6 (29)	10 (50)	
II	3 (14)	2 (10)	
III	6 (29)	0 (0)	

D

Supplemental Table 5. TSLP expression in actinic keratoses after treatment.

(**A**) Criteria used for grading TSLP protein expression in actinic keratosis (AK) at day 5. (**B**) Representative TSLP (brown) immunohistochemical (IHC) staining images of each grade are shown. (**C**) TSLP expression grades assigned blindly to actinic keratoses in calcipotriol plus 5-FU and Vaseline plus 5-FU groups are shown (corresponding to Figure 6A). (**D**) Pie charts compare the TSLP expression grades of the treated actinic keratoses in each treatment group to untreated actinic keratoses. Note that pre-treatment samples are independent of post-treatment samples. *P* value was determined by type III test of means in a mixed random effects ANOVA.

A

TSLP Expression Grades

Grade 0: No TSLP protein expression detected.

Grade I: Low TSLP expression in suprabasal keratinocytes.

Grade II: High TSLP expression in suprabasal keratinocytes or low TSLP expression in full thickness epidermis.

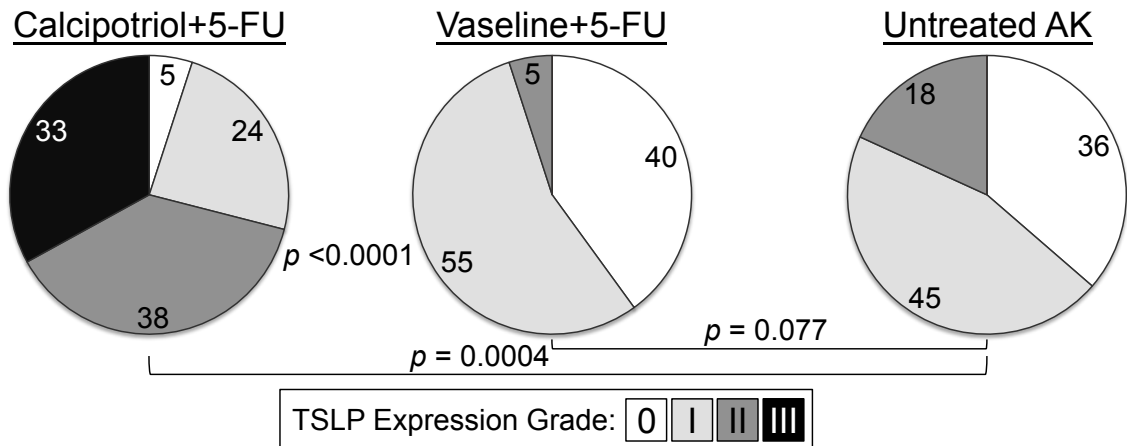**Grade III:** High TSLP expression in full thickness epidermis.

B

TSLP Expression Grades	0	I	II	III
TSLP Immunohistochemistry Example:				

C
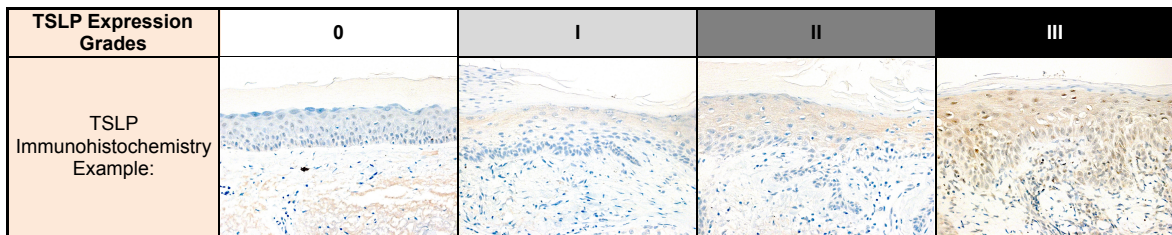
TSLP Expression Grade, no. (%)		Calcipotriol+5-FU (n = 21)	Vaseline+5-FU (n = 20)	*p value*
	0	1 (5)	8 (40)	<0.0001
	I	5 (24)	11 (55)	
	II	8 (38)	1 (5)	
	III	7 (33)	0 (0)	

D

Calcipotriol+5-FU — 5, 24, 33, 38

Vaseline+5-FU — 5, 40, 55

Untreated AK — 18, 36, 45

p <0.0001

p = 0.0004

p = 0.077

TSLP Expression Grade: 0 I II III

Supplemental Table 6. Antibodies and primers used for tissue analysis.

A

Primary Antibodies	Clone	Company
Rabbit Anti-Human CD3	2GV6	Ventana Medical Systems
Rabbit Anti-Human CD4	SP35	Ventana Medical Systems
Rabbit Anti-Human CD8	SD37	Ventana Medical Systems
Mouse Anti-Human CD56	123C3	Dako North America, Carpinteria, CA
Mouse Anti-Human HLA-DP, DQ, DR	CR3/43	Dako North America
Rabbit Anti-Human TSLP (IHC paraffin)	Polyclonal	Abcam, Cambridge, MA
Sheep Anti-Human TSLP[Biotin] (IF frozen)	Polyclonal	R&D Systems, Minneapolis, MN
Mouse Anti-Human CD20	L26	Ventana Medical Systems
Mouse Anti-Human Macrophage	HAM56	Ventana Medical Systems
Mouse Anti-Human Myeloperoxidase	59A5	Leica Biosystems, Buffalo Grove, IL
Mouse Anti-Human Cytokeratin 14 [Biotin]	LL002	Thermo Fisher Scientific, Waltham, MA
Rabbit Anti-Cytokeratin	Polyclonal	Dako North America
Mouse Anti-Human CD11c	3.9	eBioscience, San Diago, CA
Secondary Antibodies		Thermo Fisher Scientific
Goat anti-Mouse IgG, Alexa Fluor® 488 conjugate		
Goat anti-Rabbit IgG, Alexa Fluor® 568 conjugate		
Goat anti-Mouse IgG, Alexa Fluor® 647 conjugate		
Streptavidin, Alexa Fluor® 594 Conjugate		
Streptavidin, Alexa Fluor® 635 conjugate		
Chemical for Special Stains		Sigma
Toluidine Blue		
Carbol Chromotrope 2R and Phenol		

B

Gene Name	Forward Primer	Reverse Primer
MICA(9)	CACCTGCTACATGGAACACAGC	TATGGAAAGTCTGTCCGTTGACTCT
MICB(10)	ACCTTGGCTATGAACGTCACA	CCCTCTGAGACCTCGCTGCA
ULBP1(11)	GCGTTCCTTCTGTGCCTC	GGCCTTGAACTTCACACCAC
ULBP2(10)	TTACTTCTCAATGGGAGACTGT	TGTGCCTGAGGACATGGCGA
ULBP3(10)	CCTGATGCACAGGAAGAAGAG	TATGGCTTTGGGTTGAGC TAAG
IL1B(12)	CCTACTCACTTAAAGCCCGCCT	TTAGAACCAAATGTGGCCGTG
IFNB1(13)	CAGCTCCAAGAAAGGACGAAC	GGCAGTGTAACTCTTCTGCAT
MX1(13)	GACCATAGGGGTCTTGACCAA	AGACTTGCTCTTTCTGAAAAGCC
CXCL10(14)	CCAAGTGCTGCCGTCATTTTC	GGCTCGCAGGGATGATTTCAA
HMGB1(15)	AACCTATATCCCTCCCAAG	ACATCTCTCCCAGTTTCTTC
S100A8(15)	ATGCCGTCTACAGGGATGAC	ACTGAGGACACTCGGTCTCTA
S100A9(15)	GGTCATAGAACACATCATGGAGG	GGCCTGGCTTATGGTGGTG

References

1. Abel, E.L., Angel, J.M., Kiguchi, K., and DiGiovanni, J. 2009. Multi-stage chemical carcinogenesis in mouse skin: fundamentals and applications. *Nat Protoc* 4:1350-1362.

2. Cendales, L.C., Kanitakis, J., Schneeberger, S., Burns, C., Ruiz, P., Landin, L., Remmelink, M., Hewitt, C.W., Landgren, T., Lyons, B., et al. 2008. The Banff 2007 working classification of skin-containing composite tissue allograft pathology. *Am J Transplant* 8:1396-1400.

3. Velazquez, J.R., Lacy, P., Mahmudi-Azer, S., Bablitz, B., Milne, C.D., Denburg, J.A., and Moqbel, R. 2000. Interleukin-4 and RANTES expression in maturing eosinophils derived from human cord blood CD34+ progenitors. *Immunology* 101:419-425.

4. Demehri, S., Cunningham, T.J., Hurst, E.A., Schaffer, A., Sheinbein, D.M., and Yokoyama, W.M. 2014. Chronic allergic contact dermatitis promotes skin cancer. *J Clin Invest* 124:5037-5041.

5. Avants, B.B., Tustison, N.J., Song, G., Cook, P.A., Klein, A., and Gee, J.C. 2011. A reproducible evaluation of ANTs similarity metric performance in brain image registration. *Neuroimage* 54:2033-2044.

6. Mirzaalian, H., Lee, T.K., and Hamarneh, G. 2014. Spatial normalization of human back images for dermatological studies. *IEEE J Biomed Health Inform* 18:1494-1501.

7. Mirzaalian, H., Lee, T.K., and Hamarneh, G. 2016. Skin lesion tracking using structured graphical models. *Med Image Anal* 27:84-92.

8. Lian, C.G., Bueno, E.M., Granter, S.R., Laga, A.C., Saavedra, A.P., Lin, W.M., Susa, J.S., Zhan, Q., Chandraker, A.K., Tullius, S.G., et al. 2014. Biomarker evaluation of face transplant rejection: association of donor T cells with target cell injury. *Mod Pathol* 27:788-799.

9. Ritter, C., Fan, K., Paulson, K.G., Nghiem, P., Schrama, D., and Becker, J.C. 2016. Reversal of epigenetic silencing of MHC class I chain-related protein A and B improves immune recognition of Merkel cell carcinoma. *Sci Rep* 6:21678.

10. Codo, P., Weller, M., Meister, G., Szabo, E., Steinle, A., Wolter, M., Reifenberger, G., and Roth, P. 2014. MicroRNA-mediated down-regulation of NKG2D ligands contributes to glioma immune escape. *Oncotarget* 5:7651-7662.

11. Schmiedel, D., Tai, J., Yamin, R., Berhani, O., Bauman, Y., and Mandelboim, O. 2016. The RNA binding protein IMP3 facilitates tumor immune escape by downregulating the stress-induced ligands ULPB2 and MICB. *Elife* 5.

12. Monti, P., Leone, B.E., Marchesi, F., Balzano, G., Zerbi, A., Scaltrini, F., Pasquali, C., Calori, G., Pessi, F., Sperti, C., et al. 2003. The CC chemokine MCP-1/CCL2 in pancreatic cancer progression: regulation of expression and potential mechanisms of antimalignant activity. *Cancer Res* 63:7451-7461.

13. Hartlova, A., Erttmann, S.F., Raffi, F.A., Schmalz, A.M., Resch, U., Anugula, S., Lienenklaus, S., Nilsson, L.M., Kroger, A., Nilsson, J.A., et al. 2015. DNA damage primes the type I interferon system via the cytosolic DNA sensor STING to promote anti-microbial innate immunity. *Immunity* 42:332-343.

14. Lan, Y.Y., Londono, D., Bouley, R., Rooney, M.S., and Hacohen, N. 2014. Dnase2a deficiency uncovers lysosomal clearance of damaged nuclear DNA via autophagy. *Cell Rep* 9:180-192.

15. Srikrishna, G., and Freeze, H.H. 2009. Endogenous damage-associated molecular pattern molecules at the crossroads of inflammation and cancer. *Neoplasia* 11:615-628.